Class 7
Devolatilization

THF

1

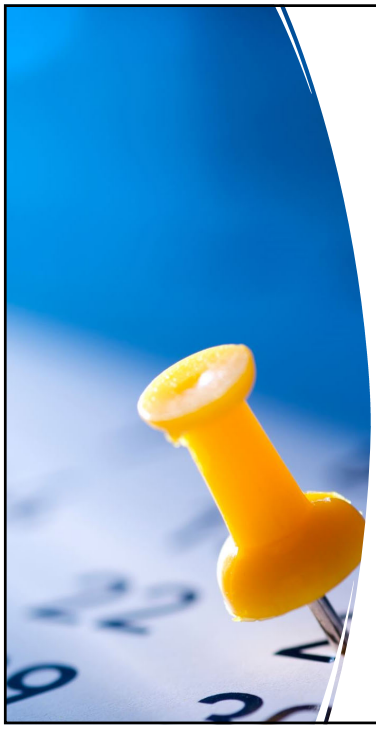

Reminder

Turn on the Zoom

2

Outline

- Equipment
- Measuring particle temperature
- Yields
  - Definitions of tar, light gas, and metaplast
  - Pressure effects
  - Heating rate effects
  - Diameter effects
  - Light gas yields
- Swelling
- Chemical composition changes during pyrolysis

3

Reading Questions

1. Please discuss the merits of the following methods for conducting devolatilization experiments: (a) thermogravimetric analyzers, (b) heated grids, (c) drop tubes, (d) flat flame burners, and (e) laser-heating of suspended particles. You may have to postulate what these reactors do if they are unfamiliar.
2. The Lee Smith book states that particle temperature is important for determining devolatilization kinetics, and that this has generally been a problem (especially at high heating rates). Please discuss why this is so important yet so difficult to measure. You may want to refer to the two most common types of rapid devolatilization experiments: drop tube reactors and heated grid reactors.
3. On p. 225, Lee Smith alludes to the fact that increases in pressure lead to decreases in tar and total volatiles yields. This can also be seen in Figure 5.110. Please explain why this happens.
4. Tom Gale (Comb. & Flame, 100, 94-100, 1995) showed how swelling decreased as heating rate increased between 10,000 K/s and 100,000 K/s for swelling coals. Please explain why swelling (a) increases with heating rate up to ~10,000 K/s and (b) decreases with heating rate after 10,000 K/s.
5. Please review the influence of the following variables on total volatiles and tar yield: (a) heating rate; (b) ambient pressure; (c) temperature; (d) coal rank; (e) particle size. Show the effect and give a brief explanation why each variable has the exhibited effect.

4

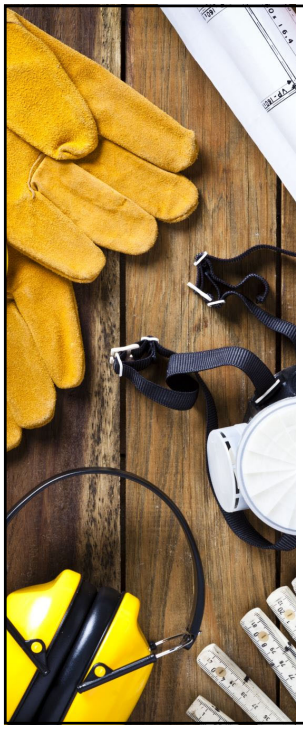

Equipment

5

TGA-FTIR

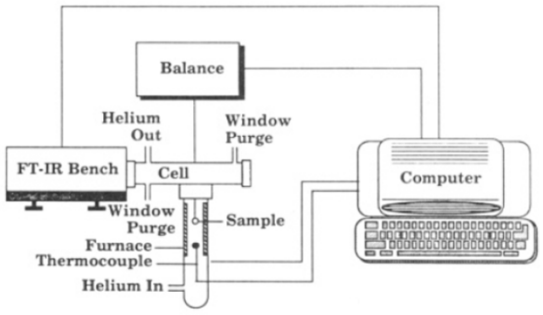

Figure 1. Schematic of TG/plus.

Solomon et al., *Energy & Fuels, Vol. 4, No. 3, 1990*

6

Heated Grid

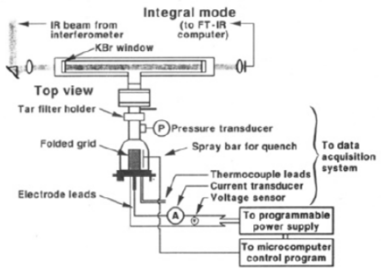

Figure 4. Heated-grid devolatilization apparatus.

Freihaut and Proscia Energy & Fuels, Vol. 3, No. 5, 1989

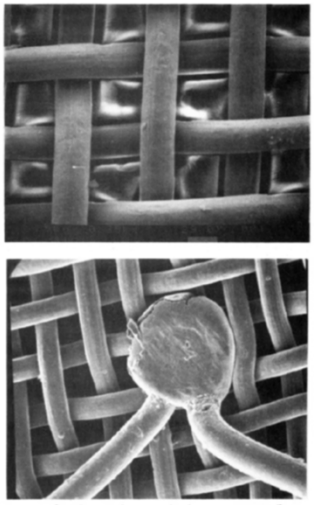

Figure 5. Stainless-steel screen: (top) screen at 315×; (bottom) thermocouple bead on screen at 245×.

7

Heated Grid

Fig. 3.3 The last development prototype reactor, assembled with the sealable trap in position. (Photo. L. Moulder)

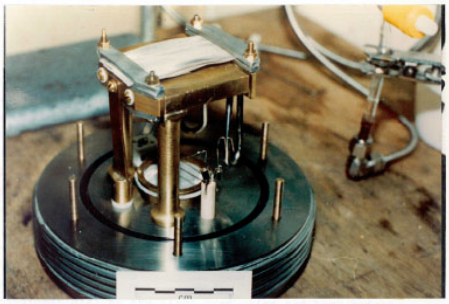

Fig. 3.26 Batch of sample holders ready for annealing.

John Gibbins Thesis, 1988

8

Heated Grid

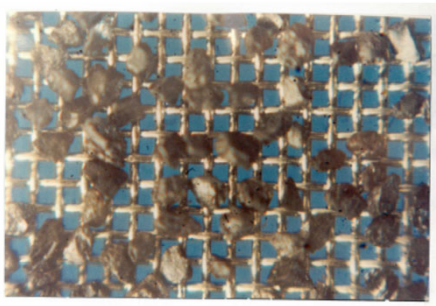

Fig. 4.22 Unfired Linby coal sample.
Refer to wire-mesh (65 micron holes) for scale.

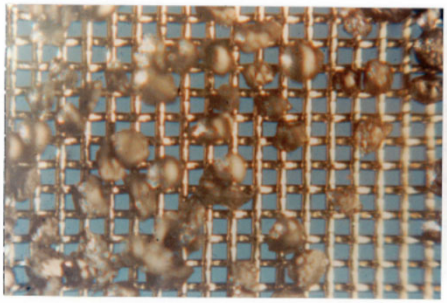

Fig. 4.23 Linby char after 1 K/s heating in helium.
Atm. press. Refer to mesh (65 micron holes) for scale.

John Gibbins Thesis, 1988

9

Drop Tube

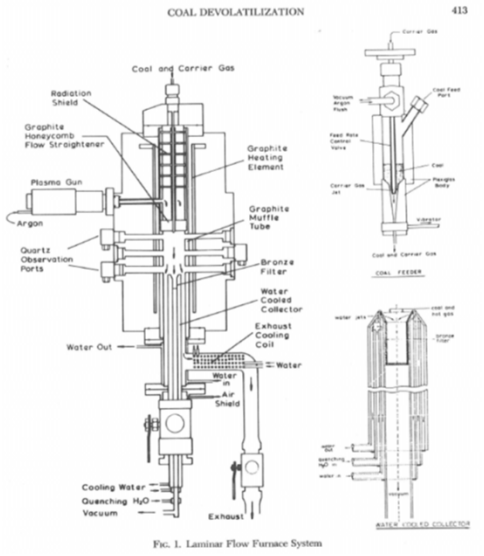

Fig. 1. Laminar Flow Furnace System

Kobayashi, et al., Comb. Inst., 16, 411-425 (1976)

10

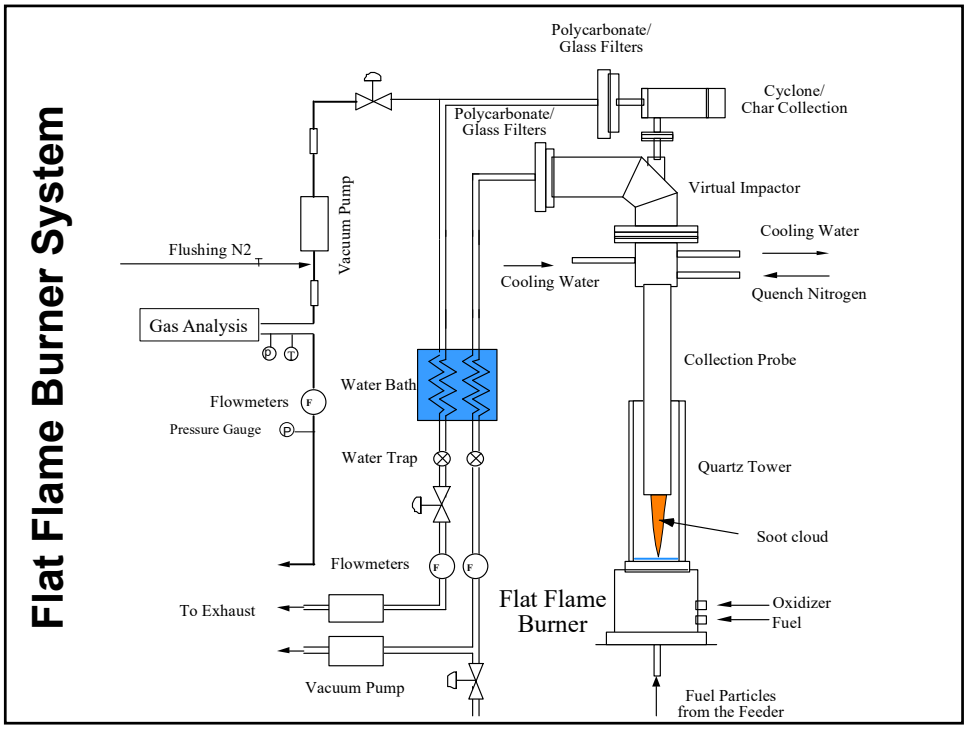
Flat Flame Burner System
Polycarbonate/
Glass Filters
Cyclone/
Char Collection
Polycarbonate/
Glass Filters
Virtual Impactor
Cooling Water
Quench Nitrogen
Cooling Water
Vacuum Pump
Flushing N2
Gas Analysis
Collection Probe
Water Bath
Flowmeters
Pressure Gauge
Water Trap
Quartz Tower
Soot cloud
Flowmeters
To Exhaust
Flat Flame
Burner
Oxidizer
Fuel
Vacuum Pump
Fuel Particles
from the Feeder

11

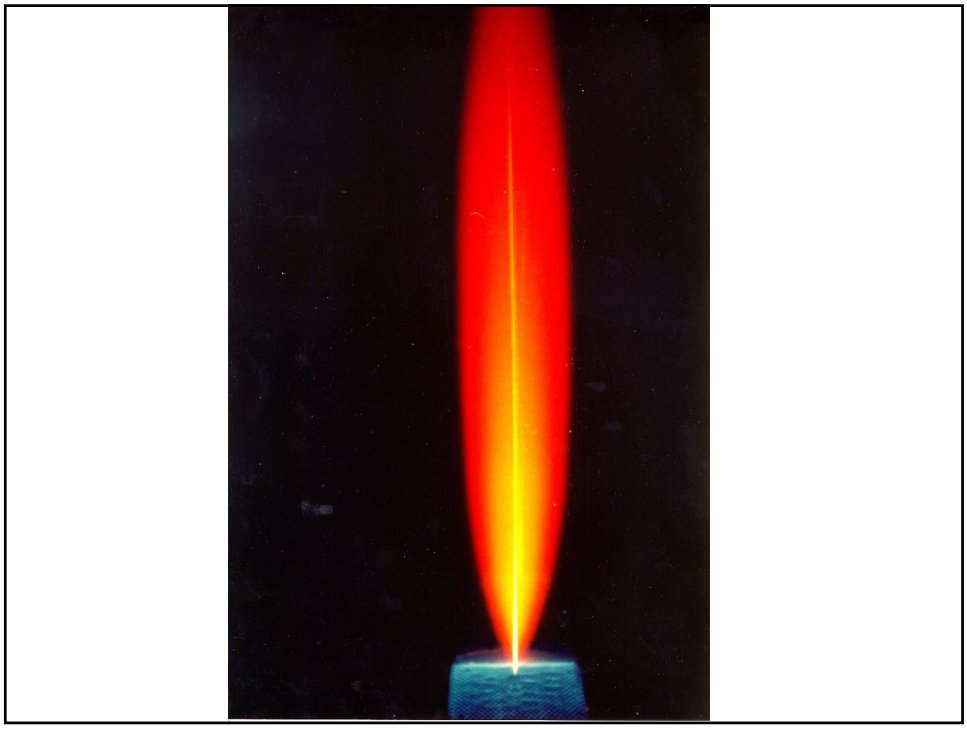

12

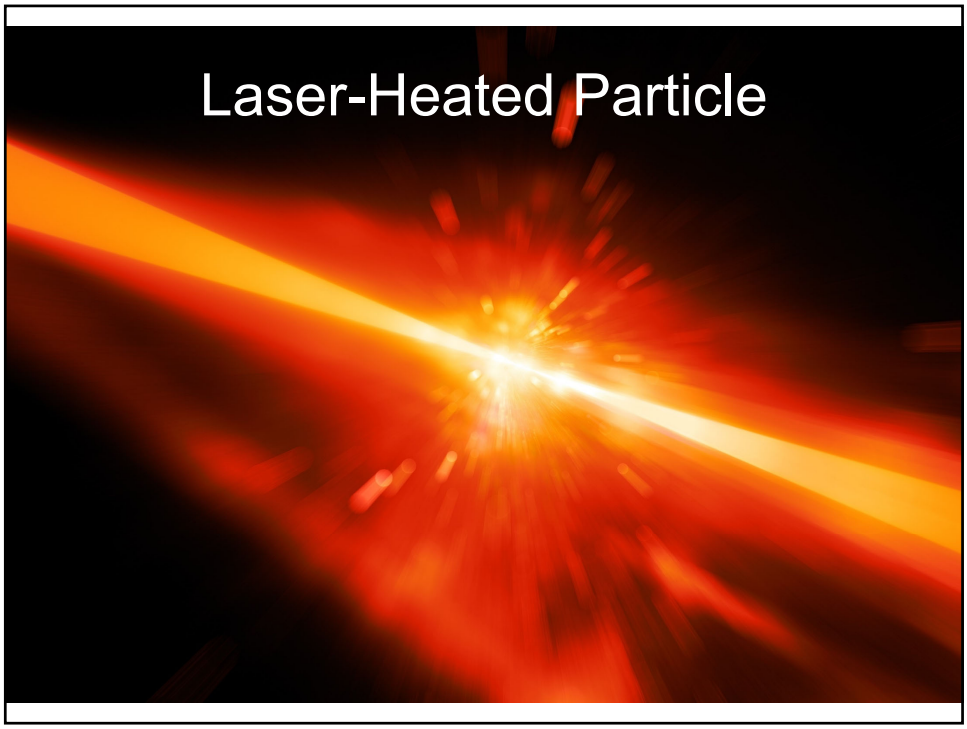

13

Pluses and Minuses of:

TGA
Heated Grid
Drop Tube
Flat-flame burner
Laser-heating of suspended particles

14

Ash Tracer Handout

15

Heated Tube Reactor

(Solomon et al., Fuel, 65, 182-194, 1986)

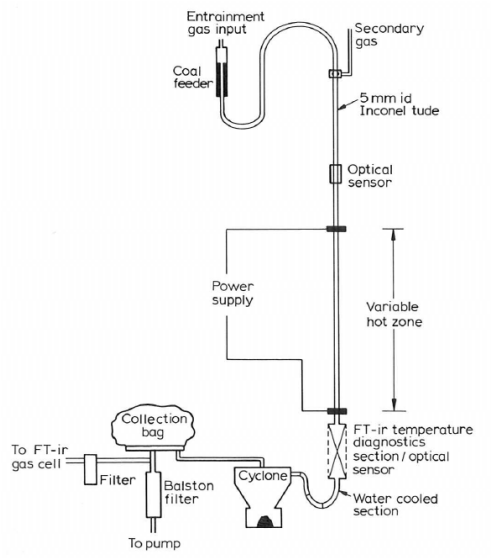

Figure 1 Schematic of heated-tube reactor

16

Devolatilization Rates

17

Wide Discrepancy Exist in Measured Rates from Heated Grids

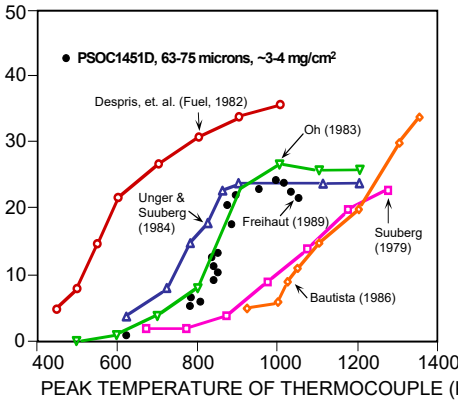

Pittsburgh hv bituminous coal, 1000 K/s, zero hold time
(from Freihaut & Proscia, Energy & Fuels, 1989)

18

Reaction Rates

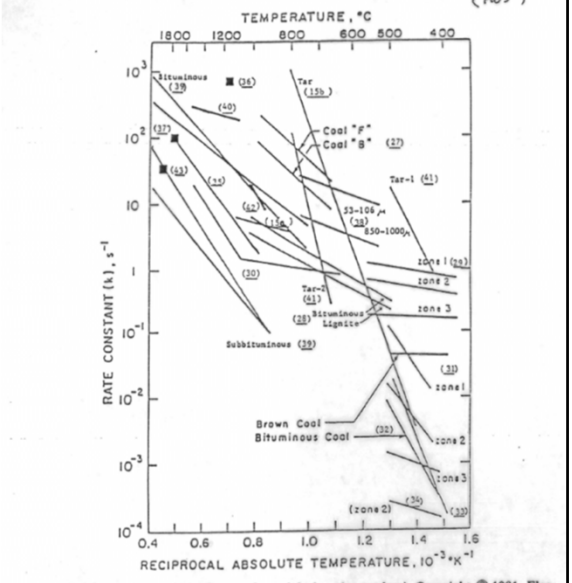

Figure 6. Comparison of kinetic rates for weight loss (or tar loss). Copyright © 1981, Electric Power Research Institute,EPRI Report No. 986-5, "Coal Devolatilization Information for Reactor Modeling," printed with permission.

19

Reaction Rates

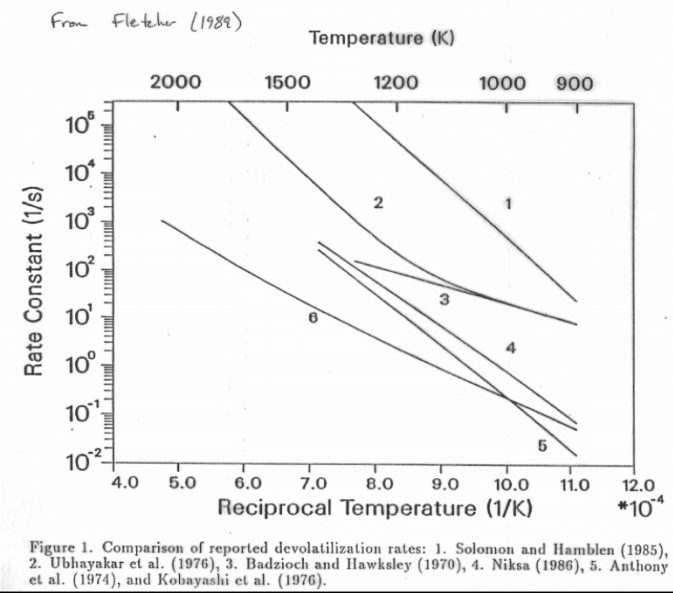

Figure 1. Comparison of reported devolatilization rates: 1. Solomon and Hamblen (1985), 2. Ubhayakar et al. (1976), 3. Badzioch and Hawksley (1970), 4. Niksa (1986), 5. Anthony et al. (1974), and Kobayashi et al. (1976).

20

Sandia Coal Devolatilization Work

Goal: Measure particle temperature during devolatilization

21

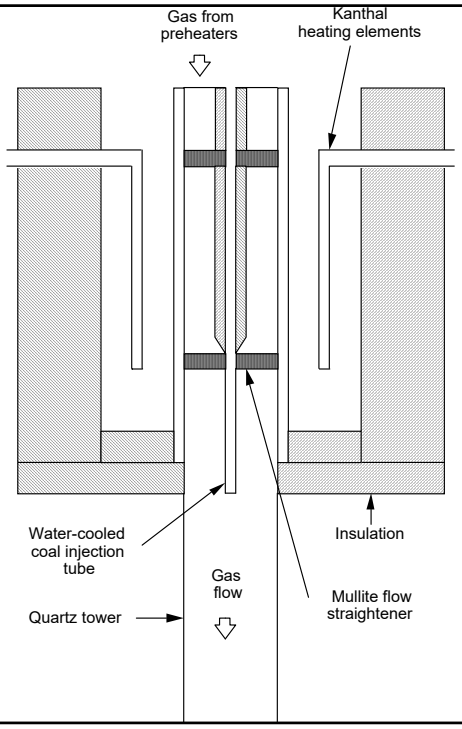

22

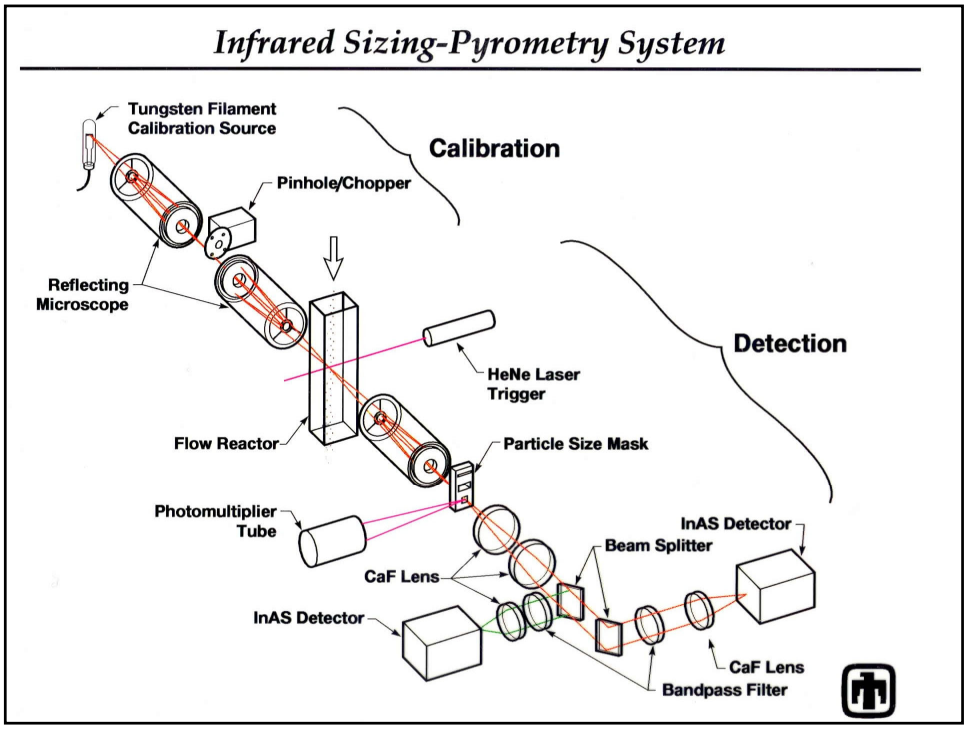
Infrared Sizing-Pyrometry System
Tungsten Filament Calibration Source
Calibration
Pinhole/Chopper
Reflecting Microscope
Detection
HeNe Laser Trigger
Flow Reactor
Particle Size Mask
Photomultiplier Tube
InAS Detector
Beam Splitter
CaF Lens
InAS Detector
CaF Lens
Bandpass Filter

23

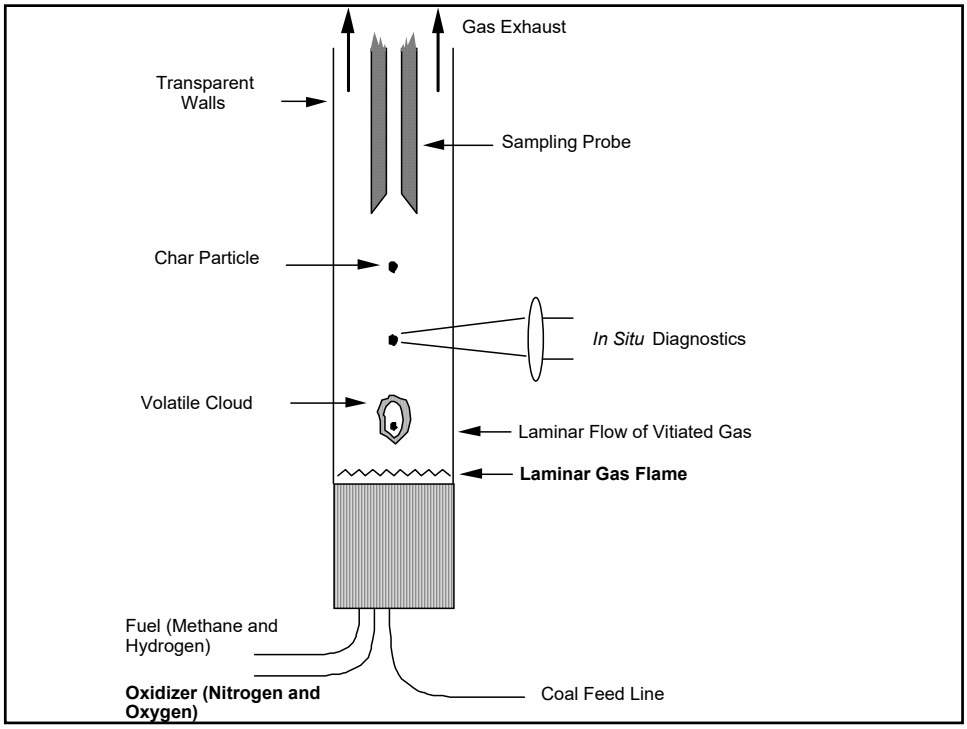
Gas Exhaust
Transparent Walls
Sampling Probe
Char Particle
In Situ Diagnostics
Volatile Cloud
Laminar Flow of Vitiated Gas
Laminar Gas Flame
Fuel (Methane and Hydrogen)
Oxidizer (Nitrogen and Oxygen)
Coal Feed Line

24

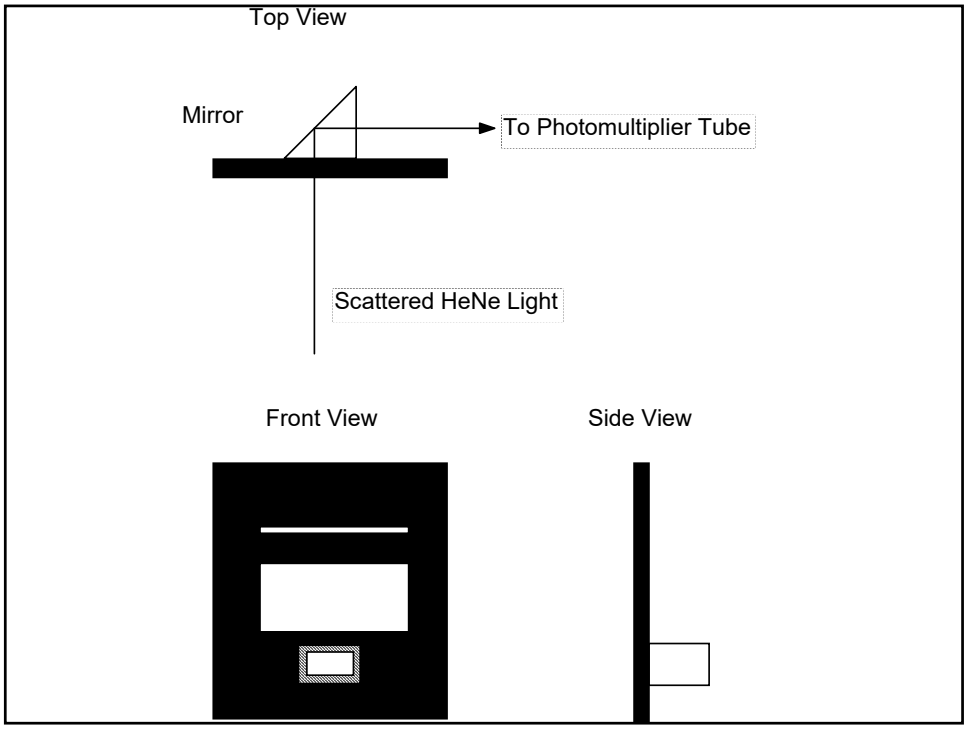
Top View
Mirror
To Photomultiplier Tube
Scattered HeNe Light
Front View
Side View

25

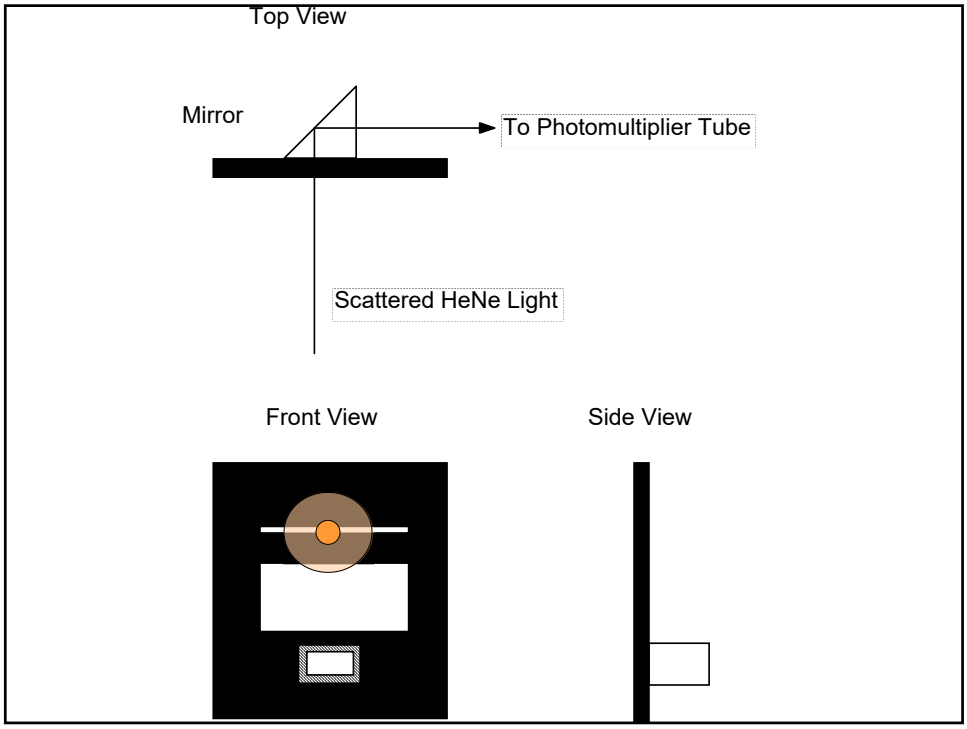
Top View
Mirror
To Photomultiplier Tube
Scattered HeNe Light
Front View
Side View

26

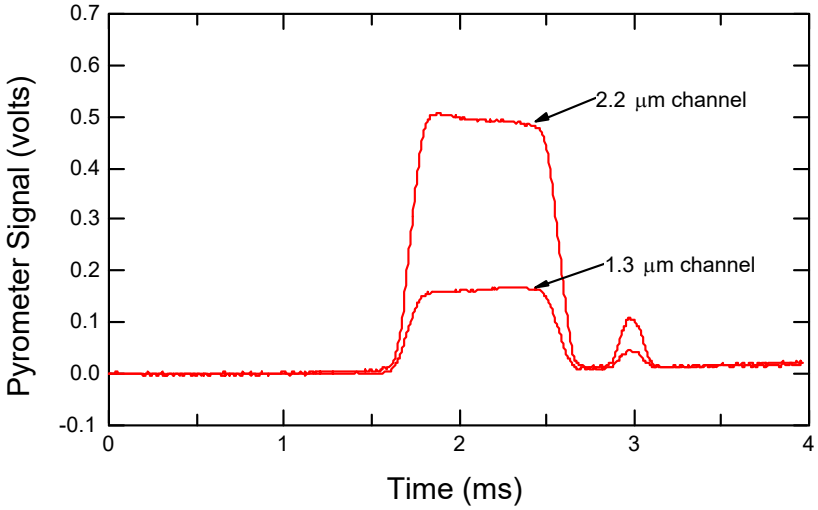

27

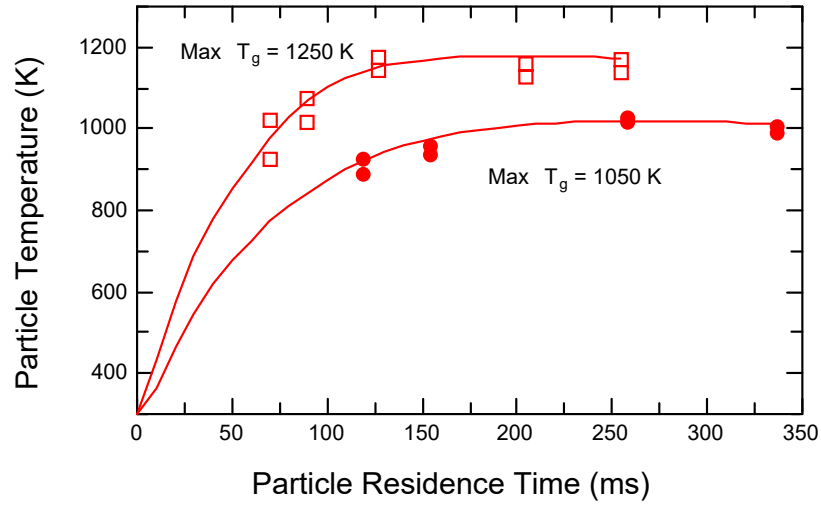

Comparison of measured (discrete points) and calculated (curves) particle temperatures as a function of residence time in the two gas conditions in the CDL for PSOC-1451 Pittsburgh #8 coal (106-125 μm size fraction). (from Fletcher, Sandia Milestone Report)

28

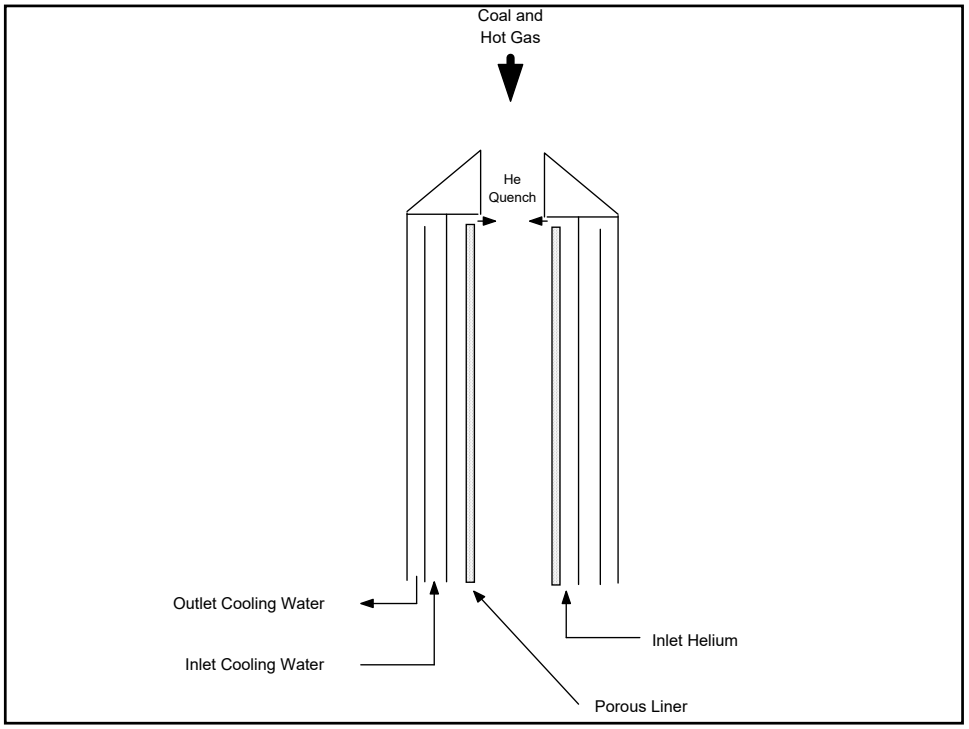
Coal and
Hot Gas
He
Quench
Outlet Cooling Water
Inlet Cooling Water
Inlet Helium
Porous Liner

29

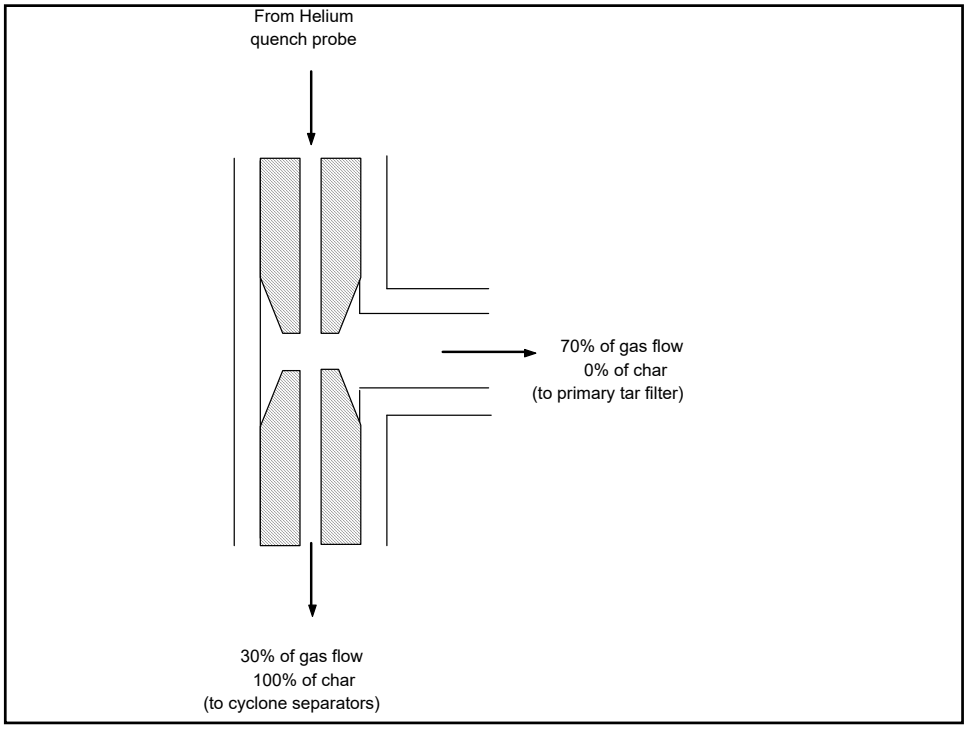
From Helium
quench probe
70% of gas flow
0% of char
(to primary tar filter)
30% of gas flow
100% of char
(to cyclone separators)

30

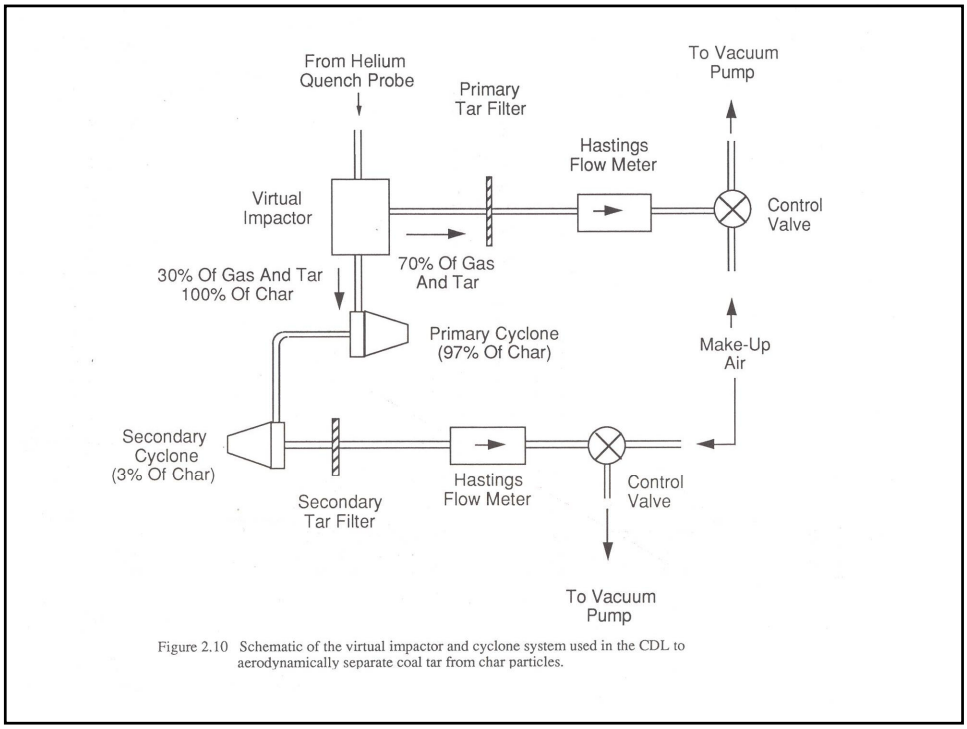

Figure 2.10 Schematic of the virtual impactor and cyclone system used in the CDL to aerodynamically separate coal tar from char particles.

31

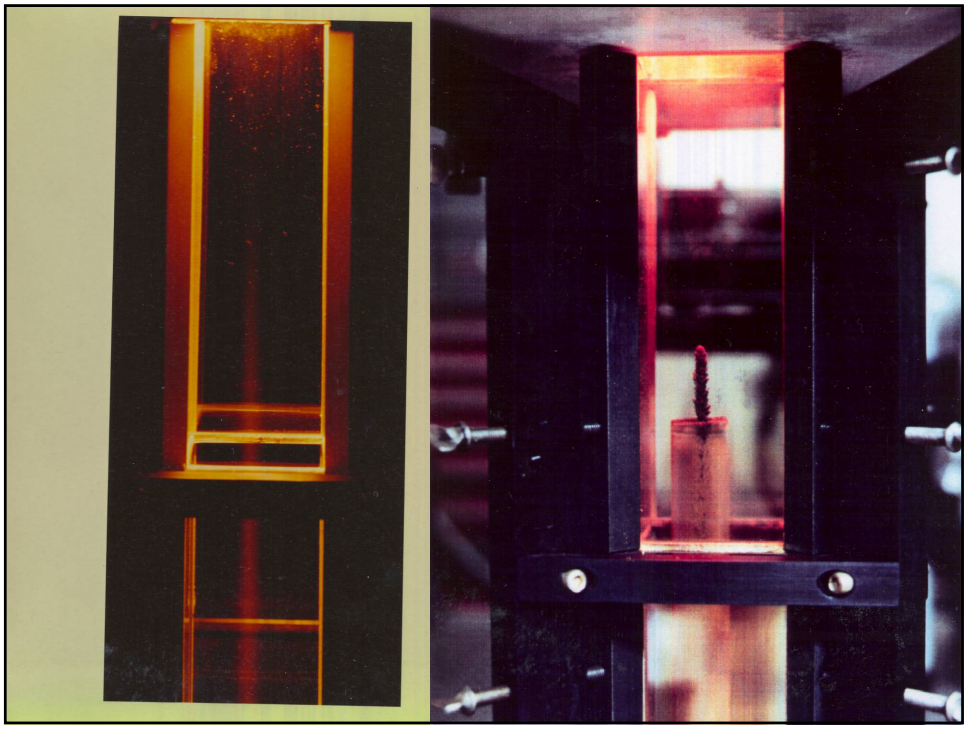

32

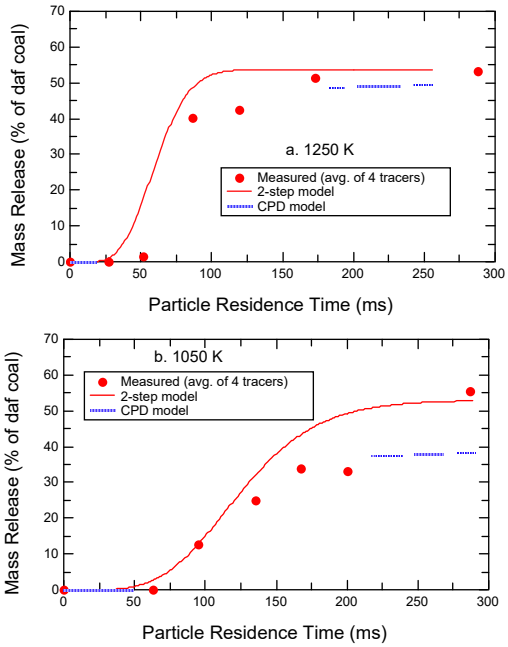

Meaured and predicted mass release as a function of residence time for PSOC-1451 hva bituminous coal particles (63-75 μm size fraction) using the 2-step model with adjusted yield coefficients and the CPD model for the (a) 1250 K gas condition and (b) 1050 K gas condition.

33

Particle Temperature Measurements During Devolatilization Improve Rate Measurements

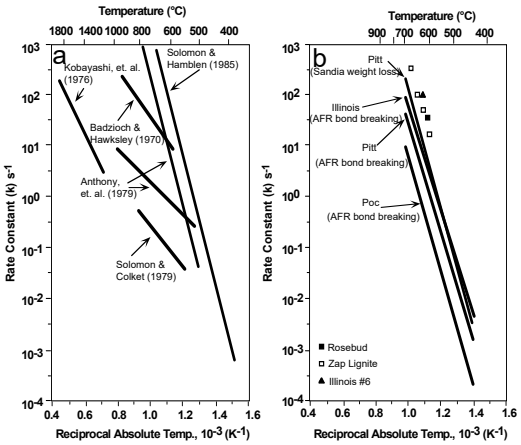

Comparison of kinetic rate constants (a) without and (b) with particle temperature measurements (from Solomon, et al., Fuel, 1993)

34

Yields

35

Definitions

- Tar = volatiles that condense at room temperature (& pressure)
- Light gas = volatiles that do not condense at room temperature (& pressure)

- Evaporation – phase change only
- Pyrolysis – bonds must break, followed by phase change

36

Comparison with ASTM Yield

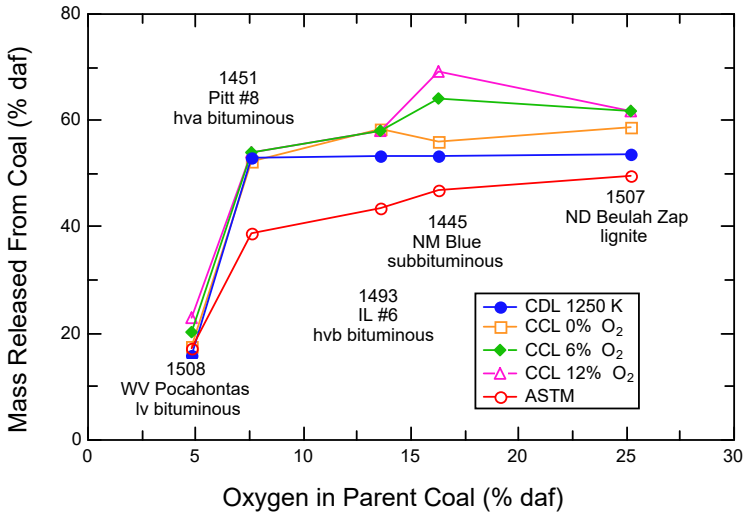

Figure 6.1 Comparison of mass release due to devolatilization in different experiments in the CDL and CCL for five PSOC-D coals. The ASTM total volatiles yields are shown for reference. The elemental oxygen level in the parent coal is used as an indicator of coal rank.

From Sandia Milestone Report, Fletcher & Hardesty (1992)

37

Tar and Total Volatile Yields Are A Function of Coal Rank

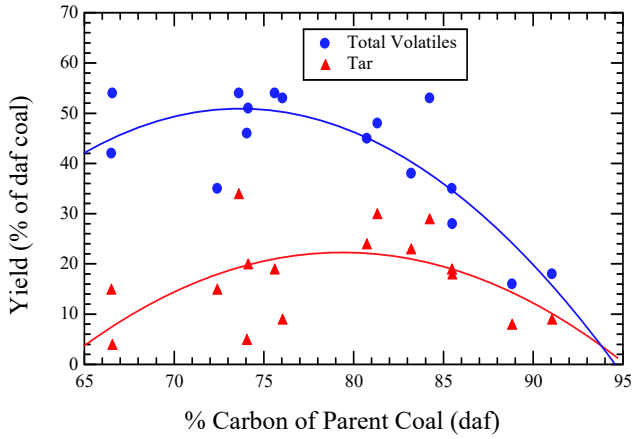

Data from TGA studies of the Argonne premium coals (Solomon), drop tube (Fletcher) and heated grid (Freihaut) studies of DOE/PETC coals

38

Total Volatile Yield Increases with Increasing Heating Rate

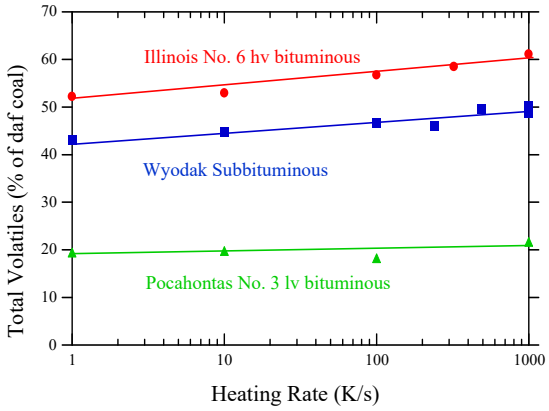

Argonne Premium coals heated to 700 °C in helium with 30 s hold (Gibbins and Kandiyoti, Energy & Fuels, 1989)

39

Reaction Temperature Increases with Increasing Heating Rate

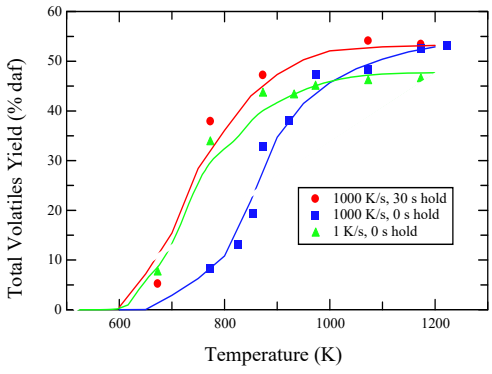

Pittsburgh No. 8 hv bituminous coal in Helium (Gibbins and Kandiyoti, E&F, 1989). Lines are CPD model predictions (Fletcher, et al., E&F 1992)

40

Particle Size Affects Yield Above ~200 μm

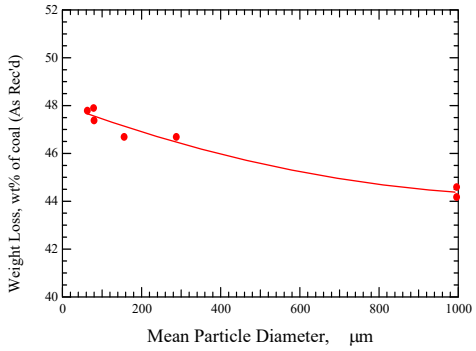

Pittsburgh hv bituminous coal in helium at 650-750 K/s to 1000 °C, 5-20 s holding time (Anthony & Howard, AIChE J, 1976)

41

Total Volatile and Tar Yields Decrease with Increasing Pressure for hv Bituminous Coals

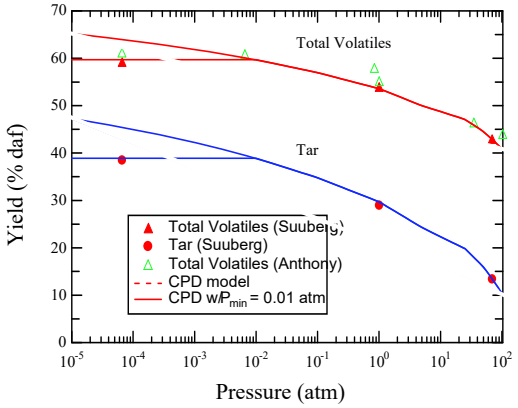

Pittsburgh hv bituminous coal data from heated grid experiments, Anthony (1974) and Suuberg (1977), 1000 K/s to 1000 °C. CPD model predictions from Fletcher, et al. (1992)

42

Effect of Pressure on Low Rank Coal Devolatilization is Small

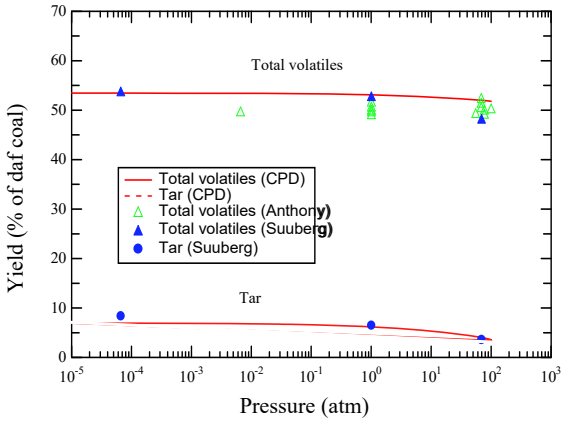

Zap lignite data from heated grid experiments, Anthony (1974) and Suuberg (1977), 1000 K/s to 1000 °C. CPD model predictions from Fletcher, et al. (1992)

43

Gas Species

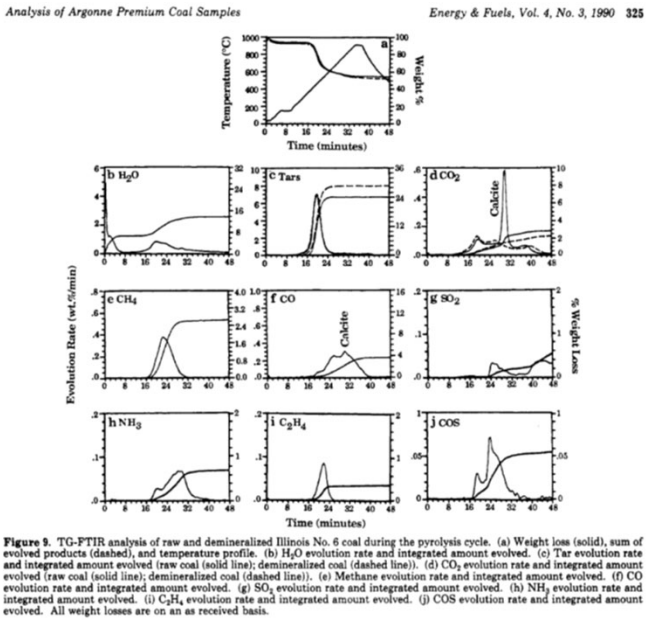

Figure 9. TG-FTIR analysis of raw and demineralized Illinois No. 6 coal during the pyrolysis cycle. (a) Weight loss (solid), sum of evolved products (dashed), and temperature profile. (b) H_2O evolution rate and integrated amount evolved. (c) Tar evolution rate and integrated amount evolved (raw coal (solid line); demineralized coal (dashed line)). (d) CO_2 evolution rate and integrated amount evolved (raw coal (solid line); demineralized coal (dashed line)). (e) Methane evolution rate and integrated amount evolved. (f) CO evolution rate and integrated amount evolved. (g) SO_2 evolution rate and integrated amount evolved. (h) NH_3 evolution rate and integrated amount evolved. (i) C_2H_4 evolution rate and integrated amount evolved. (j) COS evolution rate and integrated amount evolved. All weight losses are on an as received basis.

44

Gas Species

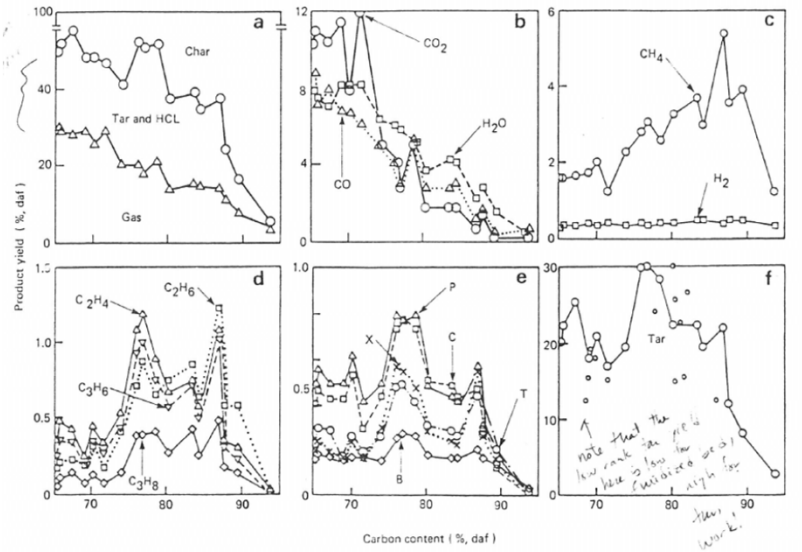

Figure 1 Effect of coal rank on yields of various products. (a) Gas including water, (tar + HCL) and char. (b) Oxygen-containing gases. (c) Methane and hydrogen. (d) C2–C3 hydrocarbons. (e) Hydrocarbon liquids: B, benzene; T, toluene; X, xylene; P, phenol; C, cresol. (f) Tar: ○. Present values: ○, Literature values

Xu & Tomita, Fuel, 66, 1987
Curie point pyrolysis, 3000 K/s to 1037 K

45

Swelling during Pyrolysis

46

Concept of Metaplast

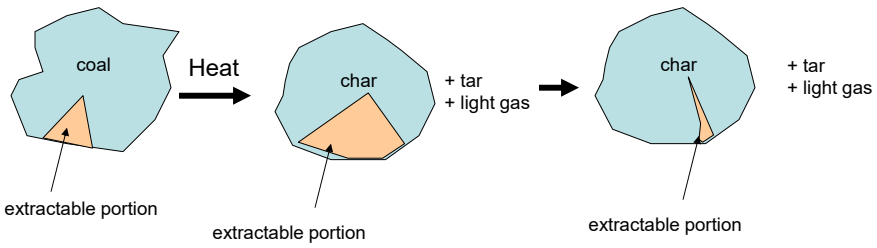

- A large pool of "liquid" material forms.
- Low molecular weight metaplast → tar
- High molecular weight metaplast → char

47

Fong Data (Fuel, 1986)

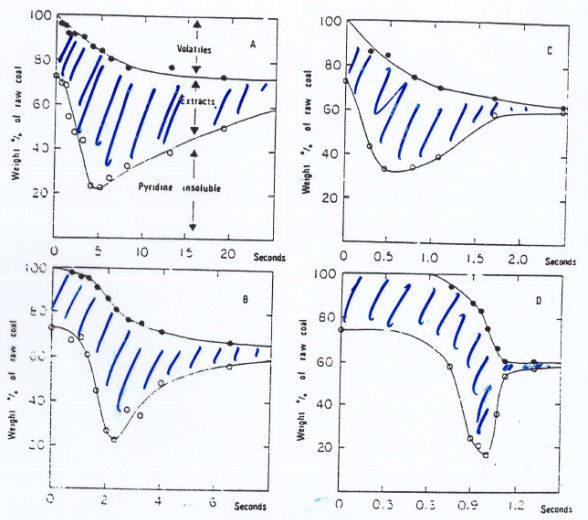

Figure 1 Volatile yields, pyridine extractables and pyridine insolubles (100% extractables volatiles) as function of temperature–time history. Parentheses indicate (heating rate, K s^{-1}; holding temperature, K; and quenching rate, K s^{-1}) A. (470,813,1100), B. (446,858,1100), C. (3300,908,4500) and D. (640,1018,1100)

Evidence for increase in extractables

48

Steam Gasification of Wyodak Coal
(2.5 atm)

- 90 ms char fully pyrolyzed
  - CPD predicts ~62% MR_{daf}
- Little change in structure from 208-868 ms
  - Linear gas temperature decrease of ~300 K from peak over 14 inches
- Highly porous chars
  - N_2 surface area of 360 m^2/g at 208 ms
- Zone II behavior near burner
  - Both d_p and ρ_p changing in first 200 ms
  - Zone III calculations predict 100% conversion in ~60 ms

90 ms

208 ms

868 ms

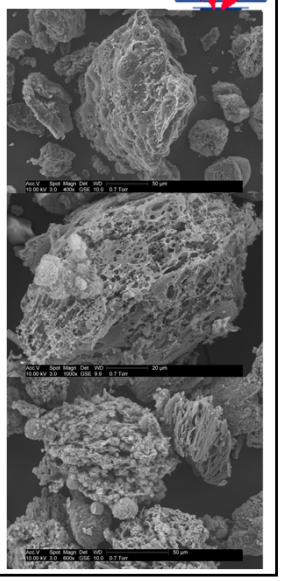

49

Pittsburgh #8 Swelling during Pyrolysis

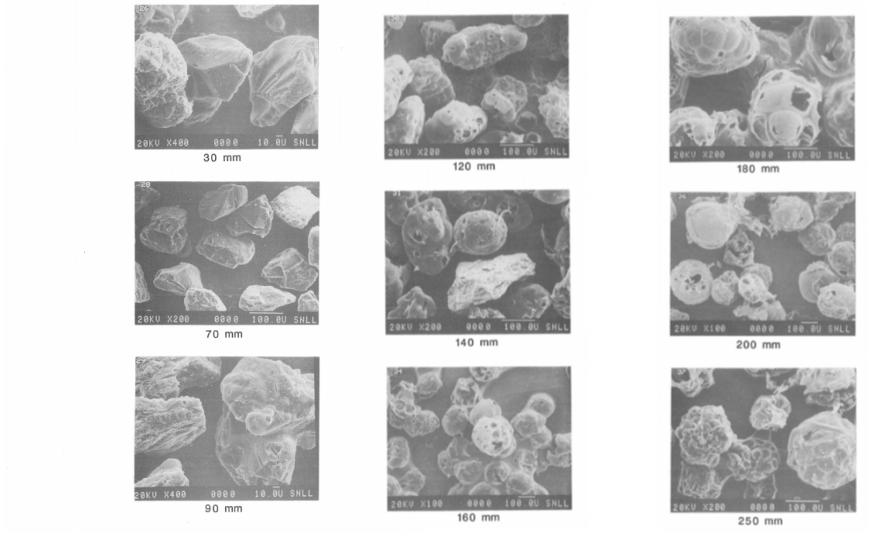

Figure 5.31 Scanning electron micrographs of 106-125 μm PSOC 1451d hva Pittsburgh bituminous coal particles collected at 30 mm, 70 mm and 90 mm from the injector for the 1050 K gas temperature condition.

50

Cross-Sections of Pitt 8 Coal during Pyrolysis

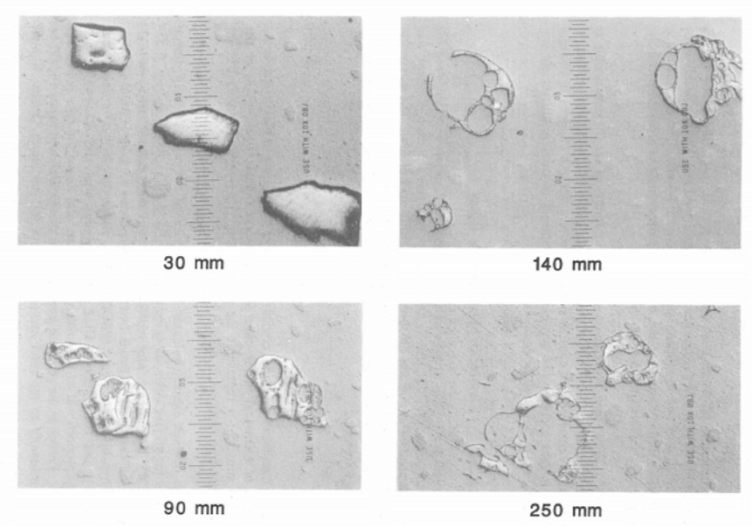

Figure 5.32 Cross-section micrographs of 106-125 µm PSOC 1451d hva Pittsburgh bituminous coal particles collected at different position in the flow reactor at the 1050 K gas temperature condition.

51

Effect of Heating Rate at 1 atm

(from Shurtz PhD Dissertation)

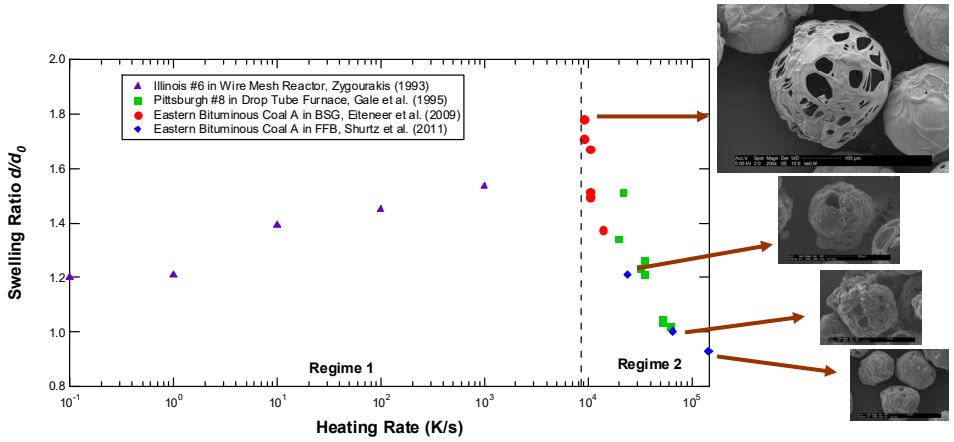

Zygourakis, K., *Energy & Fuels*, **7**(1), 33-41 (1993).
Gale, T. K., C. H. Bartholomew and T. H. Fletcher, *Combustion and Flame*, **100**(1-2), 94-100 (1995).
Eiteneer, B. et al., 26th Annual International Pittsburgh Coal Conference, Pittsburgh, PA (2009).
Shurtz, R. C., K. K. Kolste and T. H. Fletcher, *Energy & Fuels*, 25(5), 2163-2173 (2011).

52

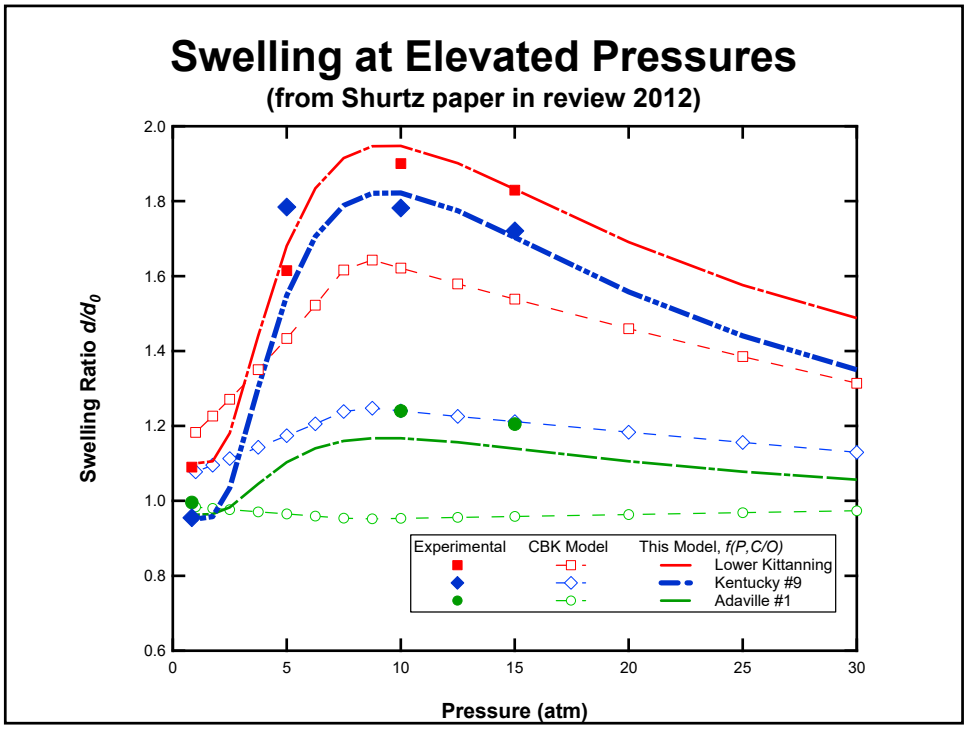
Swelling at Elevated Pressures
(from Shurtz paper in review 2012)
Swelling Ratio d/d_0
2.0
1.8
1.6
1.4
1.2
1.0
0.8
0.6
0
5
10
15
20
25
30
Pressure (atm)
Experimental
CBK Model
This Model, f(P,C/O)
Lower Kittanning
Kentucky #9
Adaville #1

53

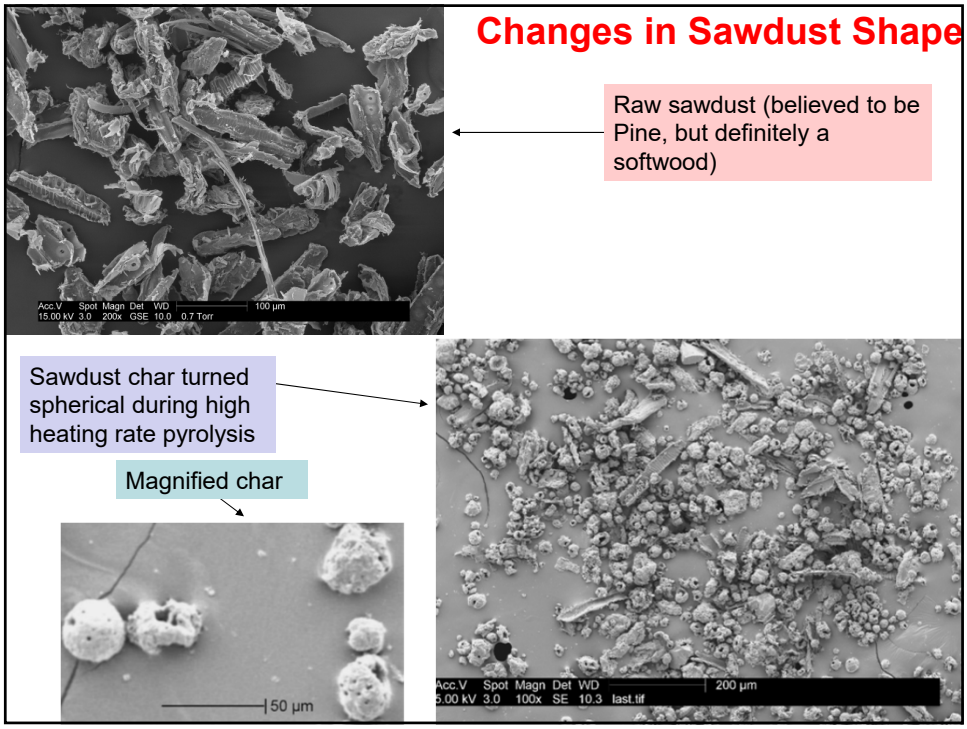
Changes in Sawdust Shape
Raw sawdust (believed to be Pine, but definitely a softwood)
Sawdust char turned spherical during high heating rate pyrolysis
Magnified char
50 µm
200 µm

54

Changes in Char Composition

55

Chemical Changes during Pyrolysis

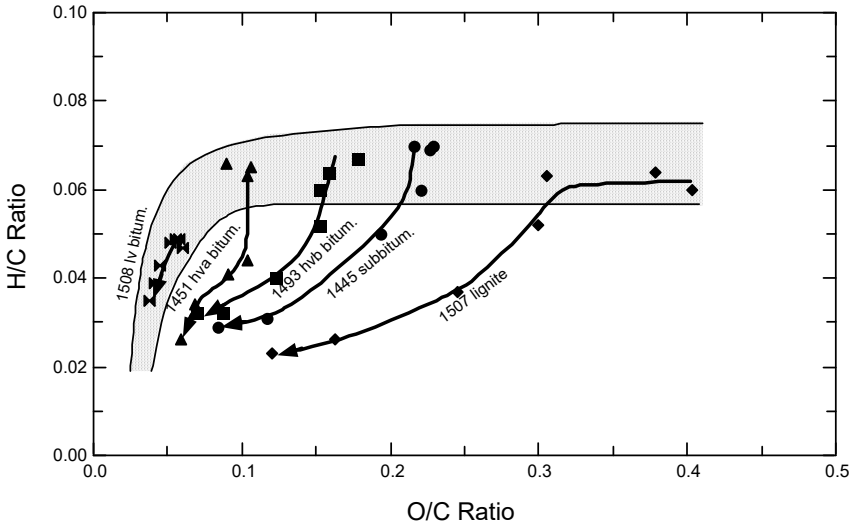

56